Spectral Analysis of Microtubule Assembly Dynamics

David J. Odde and Helen M. Buettner
Dept. of Chemical and Biochemical Engineering, Rutgers University, Piscataway, NJ 08855

Lynne Cassimeris
Dept. of Molecular Biology, Lehigh University, Bethlehem, PA 18015

Microtubules are linear polymers of the cytoskeleton that serve to organize the cytoplasm of eukaryotic cells. Understanding how microtubule polymers self-assemble is important in biotechnology, including the development of novel cancer therapies and proper guidance of regenerating neurons. The assembly of microtubules occurs by a unique process whereby an individual microtubule undergoes abrupt and apparently stochastic switching between alternating steady states of growth and shrinkage, a phenomenon known as microtubule dynamic instability. To characterize these oscillations spectral (frequency-domain) analysis, commonly used in engineering for system identification, was applied. Power spectra of the individual microtubule-length life histories revealed oscillations within growth phases, directly reflecting acceleration and deceleration in the growth process. These fluctuations were not accounted for by the standard two-state model commonly used in the analysis of microtubule assembly, despite the inclusion of simulated measurement error in the model. Thus, the spectral analysis of microtubule assembly permitted characterization of assembly process dynamics independent of particular assembly models, and as such represents a powerful analytical framework within which to study microtubule dynamic instability and assess its function in vivo.

Introduction

Microtubules are linear filaments of the cytoskeleton that organize the cytoplasm and provide communication paths between organelles (Alberts et al., 1994). Structurally, they appear as polar tubes (~ 25 nm OD, ~ 17 nm ID) with so-called plus and minus ends, the plus end being the faster growing and biologically active end. Many important cellular functions are microtubule assembly-dependent, including mitosis (Alberts et al., 1994) and axonal elongation (Daniels, 1972; Letourneau and Ressler, 1984; Tanaka et al., 1995; Yamada et al., 1970). Therefore, understanding how microtubules assemble has broad application in cancer treatment, where microtubule poisons such as taxol have been found especially potent against certain types of cancer, and possibly in directing nerve regeneration and growth by spatial and temporal manipulation of microtubule assembly within regenerating axons. It would be useful to develop a mathematical model to quantitatively describe the intrinsic dynamics of microtubules and the contribution that these dynamics make to cellular function. Ultimately, such a model could be used to identify key parameters for controlling cellular functions such as mitosis and motility.

In contrast to other self-assembling polymers, microtubules undergo abrupt transitions between alternating phases of roughly constant growth and roughly constant disassembly at steady state, with transitions occurring apparently at random as shown in Figure 1A. This process, known as dynamic instability (Mitchison and Kirschner, 1984), has been observed directly by optical videomicroscopy both in living cells (Cassimeris et al., 1988; Sammak and Borisy, 1988; Schulze and Kirschner, 1988; Shelden and Wadsworth, 1993; Tanaka and Kirschner, 1991) and *in vitro* using purified tubulin, the constituent protein of microtubules (Horio and Hotani, 1986; Walker et al., 1988). Because of the apparently random

Correspondence concerning this article should be addressed to H. M. Buettner.
Current address of D. J. Odde: Dept. of Chemical Engineering, Michigan Technological University, Houghton, MI 49931.

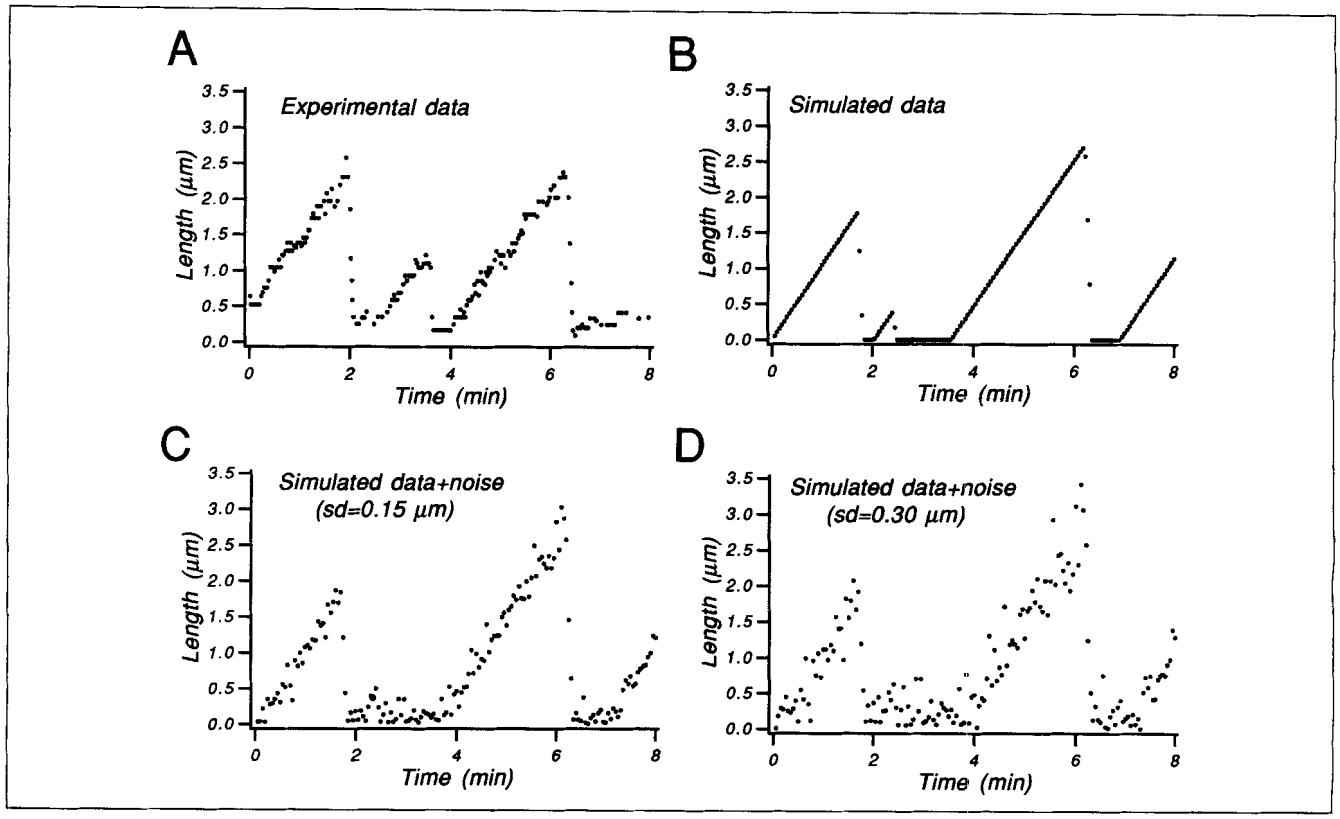

Figure 1. Experimental and simulated microtubule-length life histories.

(A) Experimental-length life history. The data resemble a "sawtooth" pattern with transitions from growth to shrinkage (catastrophes) occurring abruptly and apparently at random. Shrinkage-to-growth transitions (rescues) were rare under these conditions. Data are from the plus end assembled in 6-μM tubulin. (B) Data simulated using a two-state model. (C) Realistic ($sd = 0.15$ μm) and (D) extreme ($sd = 0.30$ μm) levels of Gaussian white noise were added to the simulated data to account for experimental measurement error.

switching, dynamic instability has been viewed as a stochastic two-state process (Bayley et al., 1989; Dogterom and Leibler, 1993; Gliksman et al., 1993; Hill, 1984; Mitchison and Kirschner, 1987; Verde et al., 1992) characterized by four parameters: the growth rate, the shrinking rate, the frequency of the growth-to-shrinkage transition (catastrophe), and the frequency of the shrinkage-to-growth transition (rescue). These parameters can be modulated *in vivo* by a number of factors (reviewed in Cassimeris, 1993), including microtubule-associated proteins (MAPs), which tend to increase the growth rate and decrease the rate of catastrophe (Horio and Hotani, 1986; Pryer et al., 1992).

While the two-state model has been useful for characterizing assembly data and simulating assembly dynamics, some results have suggested greater complexity. For example, "pauses" in dynamic instability, where microtubules neither grow nor shrink, have been observed on rare occasions in living cells (Sammak and Borisy, 1988; Shelden and Wadsworth, 1993; Tanaka and Kirschner, 1991) and *in vitro* with purified tubulin (Drechsel et al., 1992; Toso et al., 1993; Walker et al., 1988). In addition, examination of the distribution of growth times from microtubules assembled from pure tubulin *in vitro* revealed nonfirst-order catastrophe kinetics for plus ends, which in turn suggested the existence of multiple substates within the growth state (Odde et al., 1995).

The existence of microscopic substates within the growth state could also be identified by macroscopic fluctuations in the growth rate during assembly. Detecting such substates by direct observation of individual microtubules is difficult due to the superposition of experimental measurement noise on any fluctuations arising from the existence of putative substates. The strongest evidence for multiple substates has come from an analysis of growth and shrinkage rates for microtubules assembled *in vitro* from purified tubulin (Gildersleeve et al., 1992). The study found that growth and shrinkage rates varied within growth and shrinkage phases beyond that attributable to experimental measurement error. However, the analysis was limited by the somewhat arbitrary choice of a particular "window" size for estimating the rate within growth or shrinkage phases. This method requires identifying an appropriate time scale to characterize the assembly data, just as the estimation of the four parameters of dynamic instability (in the two-state model) requires identifying appropriate time scales corresponding to the mean growth time and mean shrinkage time (inverses of the catastrophe and rescue frequencies, respectively).

A more objective and general means of characterizing the fluctuations in microtubule growth rate, or any fluctuating signal, is to compute the power spectrum that quantifies the relative strength of various-sized oscillations. The presence of such oscillations may be very difficult to discern by eye in "noisy" data. In addition, spectral analysis (computing the power spectrum) allows microtubule assembly dynamics to be characterized without assuming the two-state paradigm or any

other model *a priori*. Rather than identifying particular characteristic times as is currently done, all time scales are examined for their relative contribution to the assembly dynamics. Examples of cellular and molecular processes that have been characterized by spectral analysis include fibroblast motility (Dunn and Brown, 1987), cancer cell motility (Partin et al., 1989), and ion channel conductance (DeFelice, 1981). These analyses have provided a baseline description of process dynamics, facilitated discrimination between competing models describing the process, and aided in construction of new models. In addition, spectral (or frequency-domain) analysis has been used in systems engineering (Sage and Melsa, 1971) and chemical process identification applications (Co and Ydstie, 1990). This approach has facilitated the development of process control strategies in situations where the system dynamics are "noisy" and differentiation of signals is difficult. In the present study we have applied spectral analysis to characterize microtubule-length life histories, both those obtained by direct observation of microtubules assembled from purified tubulin *in vitro* and those obtained by Monte Carlo simulation using the two-state model. The analysis permits characterization of system dynamics in a model-independent manner, and thus provides a new analytical framework within which microtubule assembly can be studied.

Materials and Methods

Tubulin and Axoneme Preparation. Porcine brain tubulin was purified by two cycles of assembly and disassembly, phosphocellulose chromatography, and a final assembly cycle in PEM buffer (0.1-M Pipes, 2-mM EGTA, 1-mM $MgSO_4$, 1-mM GTP, pH 6.9) supplemented with 1 M glutamate (Walker et al., 1988). The tubulin pellet was resuspended in PEM buffer, clarified, and stored at -75°C. One tubulin preparation was used for all the experiments. No microtubule-associated proteins were detected by silver staining of overloaded SDS-PAGE (50 μg/lane; Walker et al., 1988). Tubulin concentrations were determined as previously described (Drechsel et al., 1992). Before each experiment, a small aliquot of tubulin was thawed, stored on ice, and used within 1–2 hours. Axoneme fragments from *S. purpuratus* were purified as previously described (Walker et al., 1988) and stored at -20°C in 50% glycerol and washed in PEM buffer before use.

Microtubule Assembly. Axoneme fragments were allowed to adhere to a glass coverslip in a humid chamber for 5 min. The coverslip was then sealed onto a glass slide along the top and bottom edges with valap (1:1:1 petroleum jelly, lanolin, and paraffin) using parafilm pieces as spacers (~ 150 μm thickness). This chamber (volume ~ 15 μL) was flushed with 80 μL of PEM buffer followed by perfusion of 80 μL of 6-μM tubulin in PEM buffer. The two remaining edges of the coverslip were then sealed with Valap and the assembly mounted on the microscope for imaging of individual, nucleated microtubules.

Videomicroscopy. The assembly of individual, axoneme-nucleated microtubules at 35°C was observed by video-enhanced differential interference contrast (VE-DIC) microscopy (Salmon et al., 1989; Schnapp, 1986). A Nikon microphot-SA equipped with a 60x/1.4 NA DIC Plan Apo lens, DIC prisms, and 1.4 NA condenser was used (Vasquez et al., 1994). Illumination was provided by a 100-W mercury lamp passed through an Ellis light scrambler (Technical Video, Woods Hole, MA). The microscope stand was also equipped with heat-absorbing and 546-nm interference filters. Images were projected through a 5x projection lens to a Hamamatsu C-2400 newvicon video camera. Images were further enhanced using an Argus 10 (Hamamatsu) image processor for real-time, two-frame exponential averaging. The processed signal was passed through a time date generator (For-A Corp.) and recorded onto super VHS video tapes (Sony SV0-9500MD). An Air Stream Stage Incubator (Nicholson Precision Instruments) was used to maintain a constant temperature of 35°C on the stage (a period of 15 min was allowed to permit chamber warmup). No sample was observed longer than 1 hour.

Data Analysis. Length life histories were generated from videotapes with the use of the program RTM (courtesy of E. D. Salmon) running on an IBM PC-clone (Zenith 420 Sn) as previously described (Salmon et al., 1989). Briefly, the position of the microtubule tip was pointed to on a computer screen using a mouse-driven cursor. The operator clicked on the mouse button to record the base position of the microtubule and then clicked the mouse button at regular intervals to record the microtubule length. We estimated the spatial resolution of this system to be ~ 0.15 μm, in agreement with previously published results (Gildersleeve et al., 1992; Walker et al., 1988). The average time interval between data points, Δt, was ~ 3.0 s. Only data sets having 64 or more points were included in the analysis. Microtubule polarity was determined by the growth rate as previously described (Walker et al., 1988). The mean growth time and its standard deviation was estimated by recording the duration of each growth phase. These statistics could not be obtained for shrinkage times since nearly all of the shrinking excursions ended in complete disassembly rather than rescue. Instead, the mean shrinkage time was estimated as previously described by summing the time spent shrinking and dividing by the number of rescues (Walker et al., 1988). Spectra were estimated for each data set using the PERIOD algorithm for unevenly spaced data (Press et al., 1992). [Note that time series were stationary in the mean, since microtubules were always observed to undergo catastrophe (Odde et al., 1995).] The power spectrum for a given tubulin concentration and microtubule polarity was estimated by a weighted average of individual spectra.

Deviations from Linear Growth. A growth phase having duration ~ 3 min was chosen at random from each of three tubulin concentrations (6, 10 and 13 μM) and a given polarity (plus or minus) resulting in selection of six growth sequences altogether. A line was fitted to the length/time data by linear least-squares regression and subtracted to yield a time series of deviations from linear growth. The spectrum of each set was computed and compared to the expected spectrum for a Gaussian white noise process (independent, identically Gaussian distributed deviations). The spectral estimates were normalized so that the expected values for the white noise were equal to unity.

Two-State Simulation. Microtubules were simulated as previously described (Odde and Buettner, 1995). Briefly, four assembly parameters were defined: the growth and shrinkage rates (V_g and V_s, respectively) and the mean growth and

shrinkage times (t_g and t_s, respectively). In addition, a gamma distribution shape parameter was defined for both the growth and shrinkage time distributions (r_g and r_s, respectively; see Eq. 1). Finally, a mean nucleation time, t_n, was defined as the mean time required for a microtubule to initiate from a vacant nucleation site (assumed exponentially distributed). Growth and shrinkage times were selected at random from the gamma distribution, the cumulative distribution function of which is given by

$$F(t) = \int_0^t \frac{\theta^r t^{r-1} e^{-\theta t}}{\Gamma(r)} dt \qquad (1)$$

with parameters r and θ. Simulated-length life histories were generated by taking growth and shrinkage times randomly selected from the gamma distribution and using the growth and shrinkage rates to calculate the length at successive instants. If a microtubule completely disassembled, the vacant microtubule nucleation "site" remained empty until a new microtubule initiated at random (each nucleation time chosen randomly from the nucleation time distribution). Since the kinetics of microtubule nucleation from axoneme fragments are virtually unknown, an exponential distribution (with mean nucleation time, $t_n = 30$ s) was assumed. Sensitivity analysis showed that the power spectrum was insensitive to changes in t_n. Uncorrelated Gaussian white noise was added to each value in the length series by random selection of deviates from a standard normal distribution. A standard deviation of 0.15 μm was considered reasonable for this distribution based on previous workers' estimates using a similar experimental system (Gildersleeve et al., 1992) and visual comparison of experimental- and simulated-length life histories (Figure 1). To account for the possibility of visual filtering by the mouse–cursor operator, which might minimize the variability, a standard deviation of 0.30 μm was also used. The power spectrum of the simulated-length life histories was calculated using the same data set sizes as obtained experimentally. The simulation was performed 1,000 times and the spectra averaged to obtain the final estimate of the power spectrum.

Results

Microtubule-Length Life Histories. Microtubules were assembled *in vitro* from purified tubulin using axoneme fragments as nucleating structures. The length life histories obtained by VE-DIC microscopy and digital image analysis exhibited the sawtooth pattern characteristic of dynamic instability as shown in Figure 1A. The sawtooth pattern was also produced by the two-state simulation model, as shown in Figure 1B. Simulated measurement noise was added to each simulated data point by adding a randomly selected value from a standard normal distribution, which permitted direct comparison between experiment and model prediction. A standard deviation of 0.15 μm (Figure 1C) is a roughly realistic level of noise (Gildersleeve et al., 1992). For comparison, a standard deviation of 0.30 μm (Figure 1D) is clearly too large compared to the experimental data (Figure 1A).

Spectra of Microtubule-Length Life Histories. Microtubule-length life histories were characterized by computing the power spectrum for both microtubule polarities (plus and minus ends) at 6-μM tubulin as shown in Figure 2. In both cases there was no evidence of a dominant frequency of oscillation. Rather, spectra were broad, decaying roughly as an inverse power-law given by

$$S(f) \sim f^{-a}, \qquad (2)$$

where S is the power, f the frequency, and a the power-law exponent. The value of a, over the frequency range 0.1–5.0 min^{-1}, was 1.2 for plus ends and 1.1 for minus ends. Fitted lines reflecting the power-law decay are shown above the spectra in Figure 2. Superimposed on the experimental spectra are the spectra predicted by the two-state assembly model,

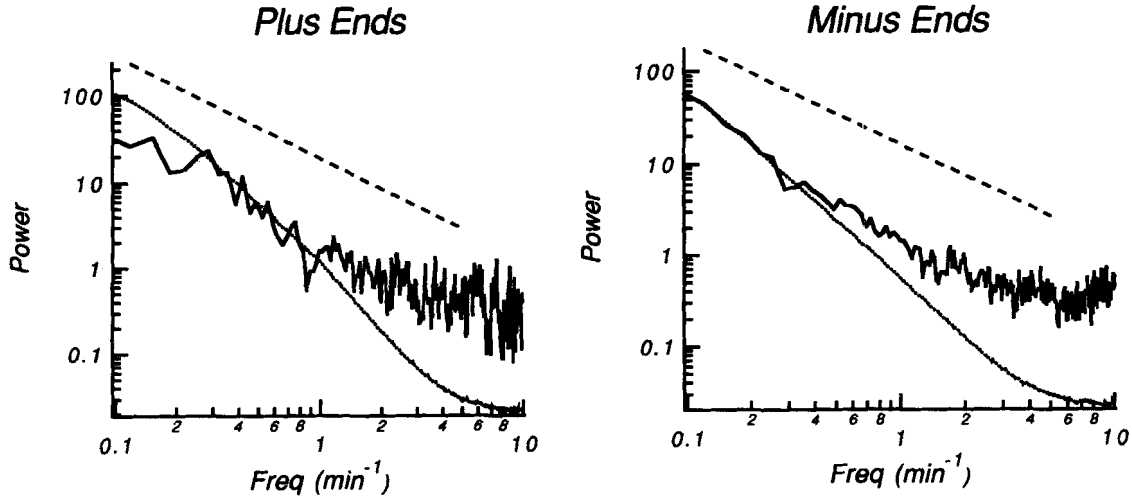

Figure 2. Spectra of microtubule-length life histories and comparison to microtubules simulated using the two-state model.

Experimental spectra (——) do not reveal any particular frequency of oscillation, but instead exhibit a broad distribution that roughly decays with frequency as an inverse power-law with slope ~1.2 for plus ends and ~1.1 for minus ends (frequency range 0.1–5.0 min^{-1}). The best-fit inverse power-law functions (– – –) are superimposed, offset above the experimental spectra by a factor of 10 for clarity. Simulated spectra (· · · ·) agree reasonably well at lower frequencies (< ~1 min^{-1}), but deviate at higher frequencies despite the inclusion of realistic levels of measurement error (sd = 0.15 μm) in the simulation.

Table 1. Dynamic Instability Parameters

	V_g μm/min	V_s μm/min	t_g min	t_s min	Δt s	N
Plus end	1.04±0.20	17.9±4.4	1.91±1.19	1.60	3.0	2,984
Minus end	0.51±0.17	23.6±13.8	3.88±2.92	1.68	3.0	7,974

6-μM tubulin, 35°C.
Data are ± *sd* (not determined for t_s).

assuming the parameters given in Table 1. The model parameters were independently estimated from the experimental data and not adjusted to improve the fit to the experimental spectrum. Below frequencies of ~ 1 min^{-1}, these spectra agreed reasonably well with spectra predicted by the two-state model. However, above frequencies of ~ 1 min^{-1} the model underpredicted the power spectrum, even though realistic experimental measurement noise levels were added to the simulated data ($sd = 0.15$ μm).

Effect of Nonexponential Phase Time Distributions. Although exponential phase time distributions are generally assumed in the literature (at least implicitly by assuming first-order catastrophe kinetics), we have found that, under the present conditions (6-μM purified tubulin), the distribution of growth times is nonexponential for plus ends (Odde et al., 1995). Accordingly, we modified the two-state model and used a gamma distribution (Eq. 1), which provided a reasonable fit to the data, to model the growth and shrinkage time distributions for plus ends. Using the previously determined best-fit value of the gamma distribution shape parameter $r = 3$ in the plus end simulation, the apparent deviations at low frequencies between the two-state model spectrum and the experimental spectrum were eliminated as shown in Figure 3. As expected, no such deviations were apparent at low frequencies for minus ends (Figure 2), where the exponential distribution ($r = 1$) adequately describes the growth-time distribution (Odde et al., 1995). Thus the present spectral analysis is consistent with the results predicted from our analysis of growth-time distributions.

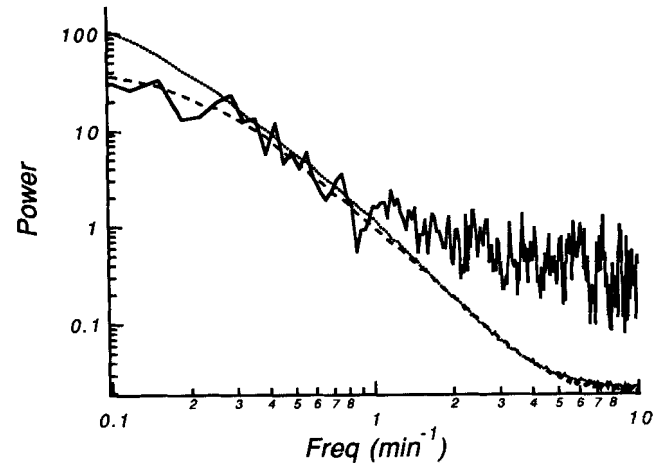

Figure 3. Effect of nonexponential phase time distributions on the plus-end spectrum.

Apparent deviations at low frequencies (~ 0.1–0.3 min^{-1}) between the experimental spectrum (——) and the simulated spectrum are eliminated when gamma distributed phase times ($r = 3$) are used in the model (– – –) instead of the commonly assumed exponential distribution (· · · ·).

Effect of Measurement Noise Levels. While the two-state model spectra provided a reasonable approximation to the experimental spectra at frequencies below ~ 1 min^{-1}, significant deviations occurred at higher frequencies (Figure 2). In an attempt to account for this deviation, an increased level of noise ($sd = 0.3$ μm) was added to the simulation. As shown in Figure 4, even this extremely high level of noise cannot account for the observed fluctuations at higher frequencies. The standard deviation of the noise level was the only model parameter that significantly affected the higher frequency portion of the power spectrum: varying any of the other simulation parameters (V_g, V_s, t_g, t_s, t_n; see Table 1) had a negligible effect on the spectrum at higher frequencies (not shown). In summary, the two-state model, although adequate

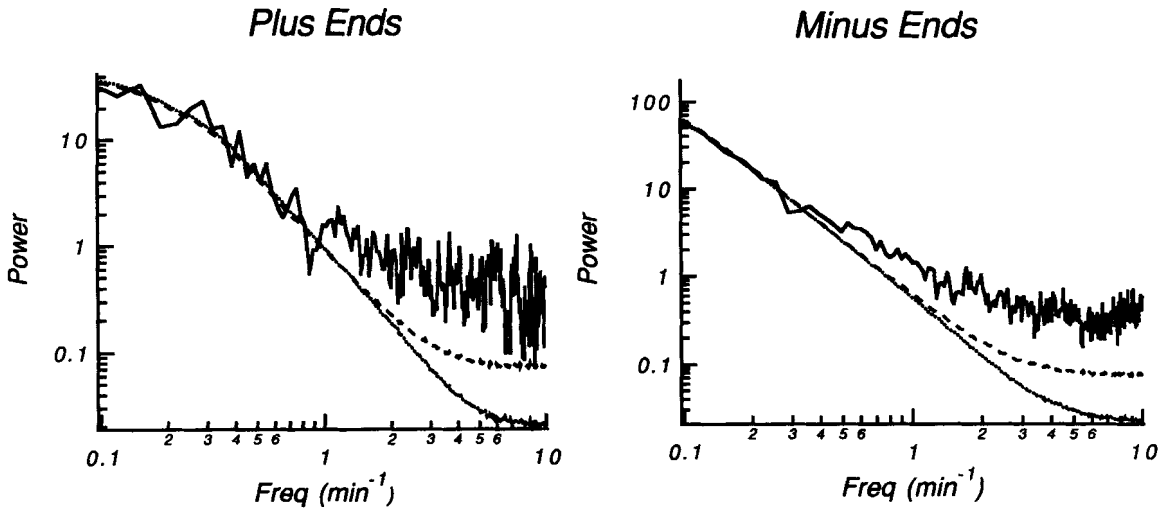

Figure 4. Effect of measurement noise levels on simulated spectra.

Despite the addition of extreme levels of measurement error to the two-state simulation (– – –; $sd = 30$ μm), the simulated spectra are unable to account for the oscillations observed experimentally (——) at frequencies above ~ 1 min^{-1}. Two-state model simulation results with a realistic level of measurement error are shown for comparison (· · · ·; $sd = 0.15$ μm).

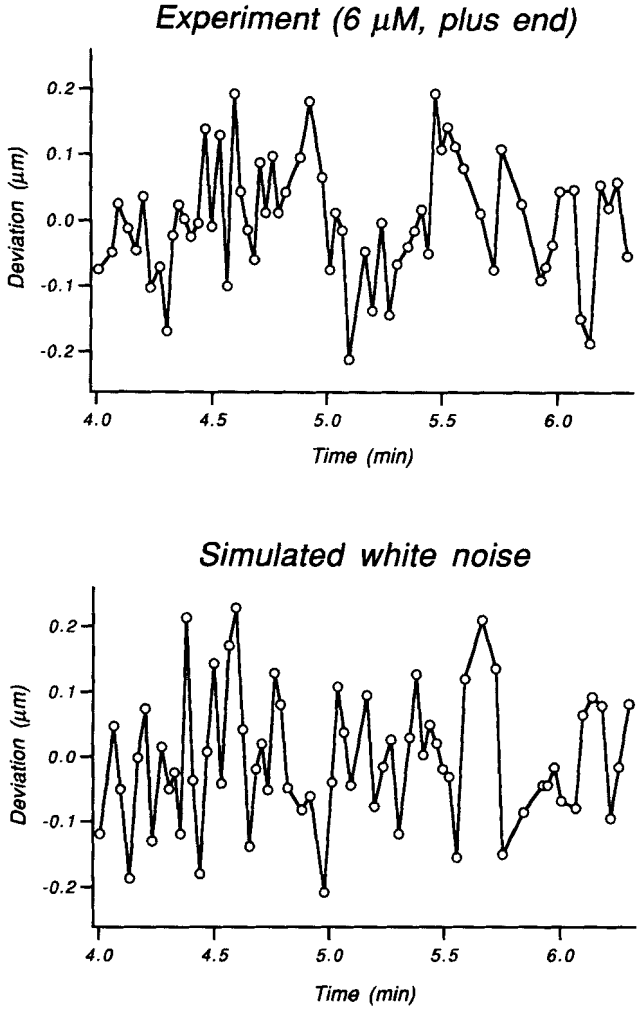

Figure 5. Example of deviations from linear growth for both an experimental growth phase (top panel) and a simulated growth phase (lower panel); both series are "noisy" with little periodicity apparent by visual inspection.

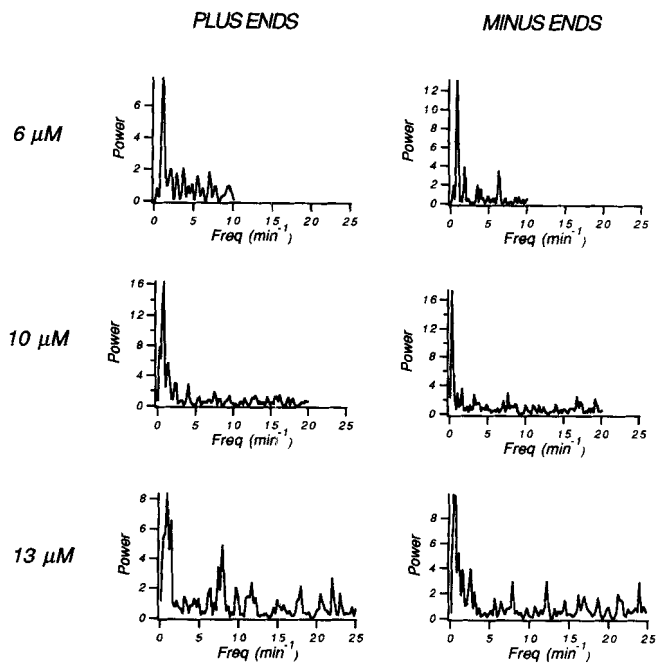

Figure 6. Power spectra of experimental deviations from linear growth.

All six randomly chosen data sets exhibited some periodicity with frequency ~ 1 min^{-1}. These results show that significant oscillations generally exist within growth phases.

for time scales longer than ~ 1 min, was not able to account for the experimentally observed fluctuations over shorter time scales even when large random measurement errors or model parameter estimation errors were included.

Deviations from Linear Growth. The deviations at higher frequencies between the experimental and two-state model spectra suggested the presence of significant oscillations within growth phases. In an attempt to identify such oscillations, a growth phase of roughly 3 min duration was chosen at random from each of three tubulin concentrations (6, 10 and 13 μM) and from each microtubule polarity (plus and minus). A line was fit to the growth data and subtracted from the data to obtain a set of deviations from linear growth. One of the resulting time series is shown in Figure 5, along with a series of simulated white noise having the same standard deviation for comparison. White noise would be expected if there were no significant periodicities within the growth phase (i.e., all the deviations away from the linear growth were due to measurement errors). However, significant oscillations in the experimental deviations from linear growth were observed in all six cases, indicating that this is a general feature of microtubule growth, as shown in Figure 6. Other peaks may represent significant oscillations as well, although each of these data sets are small ($N \sim 80$) making the significance of smaller peaks difficult to assess. The largest values of the power spectrum occurred around 1 min^{-1}, indicating that the microtubules speed up and slow down in their growth about three times within the roughly 3-min growth phases.

Discussion

The objective of the present study was to quantitatively characterize the dynamics of microtubule assembly (independent of any particular assembly model) and compare experimental data to model predictions using spectral analysis. We found that the power spectra of individual microtubule-length life histories were broad, decaying roughly according to an inverse power-law, and reasonably well-approximated by the two-state model at frequencies below ~ 1 min^{-1}. However, at frequencies above ~ 1 min^{-1}, the two-state model underpredicted the level of oscillations observed experimentally, even when experimental measurement error is accounted for. This result implies that there are significant oscillations within growth phases. By computing the power spectrum of deviations from linear growth, such oscillations were detected in six randomly chosen sets of experimental growth data. The success of the two-state model over time scales longer than ~ 1 min shows that the model represents a useful paradigm for describing the long-term evolution of microtubules undergoing dynamic instability. The failure of the two-state model over time scales shorter than ~ 1 min suggest the need for a more sophisticated model to have a full

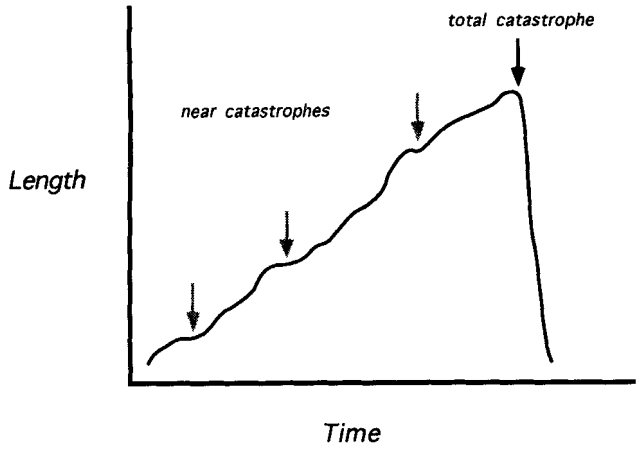

Figure 7. Model for microtubule growth near the edge of catastrophe.

Microtubules undergo occasional near catastrophes (gray arrows), one of which ultimately results in a total catastrophe (solid arrow).

description of assembly and to aid in elucidating its molecular basis.

The oscillations in microtubule length within growth phases imply that the growth rate is fluctuating, which in turn implies that, within the growth state, there are multiple substates of growth, some of which are faster growing than others. Given the apparently stochastic nature of catastrophe, it seems likely that when a microtubule's growth slows it may also be more susceptible to undergo catastrophe than when it is growing more rapidly. Thus, we propose that the oscillations detected within growth phases reflect two related features not accounted for by the two-state model: (1) multiple substates of growth and (2) occasional "near" catastrophes. These features can be incorporated into a model of assembly, depicted in Figure 7, where a growing microtubule periodically experiences "near" catastrophes, with fairly vigorous growth between these episodes, until ultimately one of these "near" catastrophes results in a complete catastrophe with the extensive subunit loss characteristic of dynamic instability. Thus, microtubules can be considered as assembling near the edge of catastrophe. The "nearness" to catastrophe is a direct reflection of the substate in which the growing microtubule exists with some substates being closer to catastrophe than others. Accordingly, a growing microtubule is not equally probable to undergo catastrophe at any instant. Rather, the probability depends on the particular substate in which the microtubule exists and possibly the pathway taken to that substate.

In support of this model we note that so-called "pause" states have been observed both *in vivo* (Sammak and Borisy, 1988; Shelden and Wadsworth, 1993; Tanaka and Kirschner, 1991) and occasionally *in vitro* with purified tubulin (Drechsel et al., 1992; Toso et al., 1993; Walker et al., 1988). These pauses may represent the largest of the "near" catastrophes, the ones that are readily apparent to the eye. Smaller "near" catastrophes are not readily detected by eye, but are detected by spectral analysis that identifies hidden periodicities in a noisy signal. In addition, variability in growth and shrinkage rates has been previously detected by computing the rate over a specified time period (window) and comparing the variability in rate to that expected from measurement error only (Gildersleeve et al., 1992). We arrived at the same result; however, the spectral analysis did not require arbitrary selection of a window size for averaging. Instead, a broad spectrum of frequencies (window sizes) was examined and the contribution of each assessed independently. Furthermore, spectral analysis permitted direct comparison of experimental assembly data to simulated assembly data without assuming a model *a priori*.

Nonfirst-Order Catastrophe Kinetics. It has often been assumed in theoretical treatments of dynamic instability that catastrophe and rescue are first-order transitions (Bayley et al., 1989; Dogterom and Leibler, 1993; Gliksman et al., 1993; Hill, 1984; Mitchison and Kirschner, 1987; Verde et al., 1992). However, probabilistic analysis showed that this is not generally the case, at least at plus ends (Odde et al., 1995). When a gamma distribution was used to model the plus end phase-time distributions in the present simulation (shape parameter $r = 3$), the simulated power spectrum collapsed onto the experimental spectrum, eliminating apparent deviations at lower frequencies (Figure 3). As expected from the growth-time distribution analysis, the standard (exponential) two-state model adequately reproduced the experimental spectrum for the minus end data, at least at frequencies shorter than ~ 1 min^{-1} (Figure 2). Thus, the present results from the spectral analysis are completely consistent with the results from the growth-time distribution analysis performed previously. Physically, the gamma distribution is consistent with a series of irreversible transitions that ultimately lead to catastrophe (Odde and Buettner, 1995; Odde et al., 1995). These transitions may correspond directly to molecular events and possibly reflect structural changes in the microtubule array.

Molecular Implications. In the present study we have simulated dynamic instability by assuming a two-state assembly model. Recently, however, a three-state model has been proposed to account for the observed behavior of microtubules that are severed in their midsection (Tran and Salmon, 1993). The model derives from the working assumption that dynamic instability is mediated by the presence or absence of a stabilizing gap of guanosine triphosphate (GTP)–tubulin subunits at the tip of the microtubule (reviewed in Caplow, 1992; Erickson and O'Brien, 1992). Briefly, GTP–tubulin subunits are incorporated into the microtubule lattice at the growing tip and subsequently hydrolyzed to GDP–tubulin and inorganic phosphate. The GTP cap model of dynamic instability holds that as long as there is a layer of GTP–tubulin subunits at the microtubule tip, the microtubule will be stable and grow. If this cap is lost, through stochastic dissociation of tubulin subunits, for example, then the labile GDP–tubulin subunits in the core of the microtubule lattice will be exposed and the microtubule will undergo rapid dissociation of GDP–tubulin subunits. According to the GTP cap model, one would expect newly exposed ends generated upon severing a microtubule in its midsection to immediately undergo rapid and extensive dissociation, presumably because the cut was made in the inner region of labile GDP–tubulin subunits. However, when microtubules are severed, either by a UV-microbeam (Walker et al., 1989) or a glass needle (Tran and Salmon, 1993), the newly exposed ends often grow instead of shrink, particularly so at newly exposed minus ends. To ex-

plain this result a three-state model was proposed where it is necessary but not sufficient to lose the GTP–tubulin cap in order for disassembly to occur. These results suggest the presence of multiple substates within the growth and shrinkage states in agreement with our conclusions drawn from the present spectral analysis.

Lateral Cap Model. The two- and three-state models of microtubule assembly are both macroscopic models that do not explicitly account for the molecular dynamics of microtubule assembly. A key advantage of molecular models is that they permit direct assessment, by computer simulation, of drug effects on microtubule assembly dynamics. Identification of key kinetic and thermodynamic model parameters can then in turn be used to develop control strategies for microtubule-dependent processes such as mitosis and motility, on microtubules. A number of quantitative, molecular models have been proposed for dynamic instability, the most viable being the Lateral Cap model, since it assumes a relatively small GTP–cap size (Bayley et al., 1990; Chen and Hill, 1983, 1985; Hill, 1987; Martin et al., 1993). While this model makes a number of assumptions that have not been experimentally tested, it nonetheless gives rise to not only nonexponentially distributed growth times (Odde et al., 1995), but also to periodic deviations from linear growth as shown in Figure 8. The period of the oscillations is roughly on the same time scale as those seen experimentally (Figure 6). Neither the two-state nor the three-state model is capable of reproducing these spectra. Therefore, the Lateral Cap model warrants further investigation as a quantitative molecular model for microtubule assembly.

Self-Organized Criticality. Microtubule dynamic instability shares a number of characteristics of a class of dynamical systems termed self-organized critical (SOC) systems (Bak et al., 1988). In these systems many interacting elements self-organize into a marginally stable state. Instead of reaching an equilibrium, the system evolves from one meta-stable state to another. Typically, the evolution of the system occurs in cascades of all different sizes, with many small events and a few large events. A prototypical example illustrating SOC behavior is a sandpile (Bak et al., 1988). Individual grains of sand are added to the pile until a critical slope is built up. When new grains are then added to the sandpile, they usually displace a couple of other grains. Occasionally, the displaced grains displace other grains, which in turn displace still more until a large number of grains cascade in an avalanche down the side of the pile. Thus, there are many small avalanches and fewer large avalanches. Besides sandpiles, the features of SOC arise in models of earthquakes, automobile traffic, forest fires, and turbulence (Bak and Chen, 1991).

Microtubule dynamic instability appears to possess some of the features of SOC systems: tubulin molecules self-organize into a microtubule that is metastable. The assembly process never reaches equilibrium, but instead switches between alternating states of growth and shrinkage. The growing and shrinking excursions are varied in size with small excursions occurring more frequently than large excursions (Odde et al., 1995). Moreover, a signature characteristic of SOC systems is that their time evolution is characterized by a power spectrum whose distribution is an inverse power-law with exponent $a \sim 1$ (also known as $1/f$ or flicker noise; Eq. 2). In this light it is intriguing that we find a roughly inverse power-law power spectrum for microtubule-length life histories with exponent $a \sim 1.1$–1.2. Such behavior has also been found for simulated coevolutionary systems and has been termed "adaptation at the edge of chaos" (Kauffman, 1993). In this context, microtubules may be exhibiting dynamics generally characteristic of exploratory and evolutionary systems.

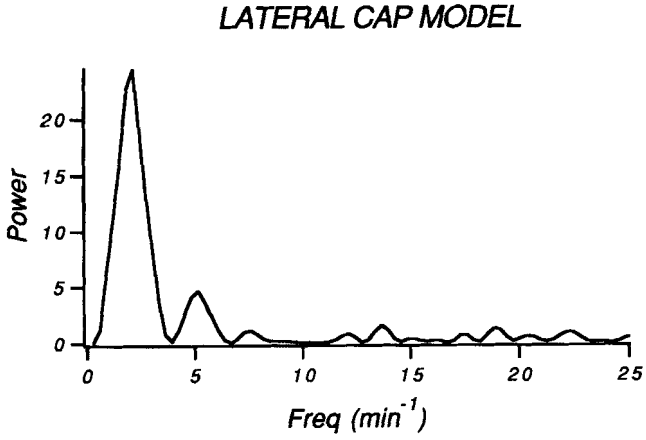

Figure 8. Power spectrum of deviations from linear growth produced by the Lateral Cap model.

Significant oscillations at a frequency of ~ 1–3 min^{-1} are repeatedly observed in reasonable agreement with the experimental results. A typical spectrum is shown.

Acknowledgments

The theoretical work was supported by a grant from the National Science Foundation to H.M.B. (BCS 92-10540). The experimental work was supported by a grant from the National Science Foundation to H.M.B. (IBN 94-09184) and a grant from the National Institutes of Health to L.C. (GM49763). The authors thank Chao Tang for helpful discussions regarding self-organized criticality and Julius Fernandez for technical assistance with the Lateral Cap simulations. Julius Fernandez was supported by an REU Supplement to NSF BCS 92-10540.

Notation

N = total number of data points in length life histories
Δt = average sampling interval
θ = gamma distribution time constant

Literature Cited

Alberts, B., D. Bray, J. Lewis, M. Raff, K. Roberts, and J. D. Watson, *Molecular Biology of the Cell*, 3rd ed., Garland Publ., New York (1994).

Bak, P., and K. Chen, "Self-Organized Criticality," *Sci. Amer.*, 46 (Jan., 1991).

Bak, P., C. Tang, and K. Wiesenfeld, "Self-Organized Criticality," *Phys. Rev. A*, **38**, 364 (1988).

Bayley, P. M., M. J. Schilstra, and S. R. Martin, "A Simple Formulation of Microtubule Dynamics: Quantitative Implications of the Dynamic Instability of Microtubule Populations in Vivo and in Vitro," *J. Cell Sci.*, **93**, 241 (1989).

Bayley, P. M., M. J. Schilstra, and S. R. Martin, "Microtubule Dynamic Instability: Numerical Simulation of Microtubule Transition Properties using a Lateral Cap Model," *J. Cell Sci.*, **95**, 33 (1990).

Caplow, M., "Microtubule Dynamics," *Curr. Opin. Cell Biol.*, **4**, 58 (1992).

Cassimeris, L., "Regulation of Microtubule Dynamic Instability," *Cell Motil. Cytoskel.*, **26**, 275 (1993).

Cassimeris, L., N. K. Pryer, and E. D. Salmon, "Real-Time Observations of Microtubule Dynamic Instability in Living Cells," *J. Cell Biol.*, **107**, 2223 (1988).
Chen, Y., and T. L. Hill, "Use of Monte Carlo Calculations in the Study of Microtubule Subunit Kinetics," *Proc. Nat. Acad. Sci. U.S.A.*, **80**, 7520 (1983).
Chen, Y., and T. L. Hill, "Monte Carlo Study of the GTP Cap in a Five-Start Helix Model of a Microtubule," *Proc. Nat. Acad. Sci. U.S.A.*, **82**, 1131 (1985).
Co, T. B., and B. E. Ydstie, "System Identification using Modulating Functions and Fast Fourier Transforms," *Comput. Chem. Eng.*, **14**, 1051 (1990).
Daniels, M. P., "Colchicine Inhibition of Nerve Fiber Formation in Vitro," *J. Cell Biol.*, **53**, 164 (1972).
DeFelice, L. J., *Introduction to Membrane Noise*, Plenum Press, New York (1981).
Dogterom, M., and S. Leibler, "Physical Aspects of the Growth and Regulation of Microtubule Structures," *Phys. Rev. Lett.*, **70**, 1347 (1993).
Drechsel, D. N., A. A. Hyman, M. H. Cobb, and M. W. Kirschner, "Modulation of the Dynamic Instability of Tubulin Assembly by the Microtubule-Associated Protein Tau," *Mol. Biol. Cell*, **3**, 1141 (1992).
Dunn, G. A. and A. F. Brown, "A Unified Approach to Analyzing Cell Motility," *J. Cell Sci. Suppl.*, **8**, 81 (1987).
Erickson, H. P., and E. T. O'Brien, "Microtubule Dynamic Instability and GTP Hydrolysis," *Ann. Rev. Biophys. Biomol. Struct.*, **21**, 145 (1992).
Gildersleeve, R. F., A. R. Cross, K. E. Cullen, A. P. Fagen, and R. C. Williams, Jr., "Microtubules Grow and Shorten at Intrinsically Variable Rates," *J. Biol. Chem.*, **267**, 7995 (1992).
Gliksman, N. R., R. V. Skibbens, and E. D. Salmon, "How the Transition Frequencies of Microtubule Dynamic Instability (Nucleation, Catastrophe, and Rescue) Regulate Microtubule Dynamics in Interphase and Mitosis: Analysis using a Monte Carlo Computer Simulation," *Mol. Biol. Cell*, **4**, 1035 (1993).
Hill, T. L., "Introductory Analysis of the GTP-Cap Phase Change Kinetics at the End of a Microtubule," *Proc. Nat. Acad. Sci. U.S.A.*, **81**, 6728 (1984).
Hill, T. L., *Linear Aggregation Theory in Cell Biology*, Springer-Verlag, New York (1987).
Horio, T., and H. Hotani, "Visualization of the Dynamic Instability of Individual Microtubules," *Nature*, **321**, 605 (1986).
Kauffman, S. A., *The Origins of Order*, Oxford Univ. Press, New York (1993).
Letourneau, P. C., and A. H. Ressler, "Inhibition of Neurite Initiation and Growth by Taxol," *J. Cell Biol.*, **98**, 1355 (1984).
Martin, S. R., M. J. Schilstra, and P. M. Bayley, "Dynamic Instability of Microtubules: Monte Carlo Simulation and Application to Different Types of Microtubule Lattice," *Biophys. J.*, **65**, 578 (1993).
Mitchison, T. J., and M. W. Kirschner, "Dynamic Instability of Microtubule Growth," *Nature*, **312**, 237 (1984).
Mitchison, T. J., and M. W. Kirschner, "Some Thoughts on the Partitioning of Tubulin Between Monomer and Polymer under Conditions of Dynamic Instability," *Cell Biophys.*, **11**, 35 (1987).
Odde, D. J., and H. M. Buettner, "Time Series Characterization of Simulated Microtubule Dynamics in the Nerve Growth Cone," *Ann. Biomed. Eng.*, **23**, 268 (1995).
Odde, D. J., L. Cassimeris, and H. M. Buettner, "Kinetics of Microtubule Catastrophe Assessed by Probabilistic Analysis," *Biophys. J.*, **69**, 796 (1995).
Partin, A. W., J. S. Schoeniger, J. L. Mohler, and D. S. Coffey, "Fourier Analysis of Cell Motility: Correlation of Motility with Metastatic Potential," *Proc. Nat. Acad. Sci. U.S.A.*, **86**, 1254 (1989).
Press, W. H., S. A. Teukolsky, W. T. Vetterling, and B. P. Flannery, *Numerical Recipes in Fortran*, 2nd ed., Press Syndicate of the Univ. of Cambridge, New York (1992).
Pryer, N. K., R. A. Walker, V. P. Skeen, B. D. Bourns, M. F. Sobeiro, and E. D. Salmon, "Brain Microtubule-Associated Proteins Modulate Microtubule Dynamic Instability in Vitro," *J. Cell Sci.*, **103**, 965 (1992).
Sage, A. P., and J. C. Melsa, *System Identification*, Academic Press, San Diego (1971).
Salmon, T., R. A. Walker, and N. K. Pryer, "Video-Enhanced Differential Interference Contrast Light Microscopy," *BioTechniques*, **7**, 624 (1989).
Sammak, P. J., and G. G. Borisy, "Direct Observation of Microtubule Dynamics in Living Cells," *Nature*, **332**, 724 (1988).
Schnapp, B. J., "Viewing Single Microtubules by Video Light Microscopy," *Meth. Enzymol.*, **134**, 561 (1986).
Schulze, E., and M. Kirschner, "New Features of Microtubule Behaviour Observed *in Vivo*," *Nature*, **334**, 356 (1988).
Shelden, E., and P. Wadsworth, "Observation and Quantification of Individual Microtubule Behavior in Vivo: Microtubule Dynamics are Cell-Type Specific," *J. Cell Biol.*, **120**, 935 (1993).
Tanaka, E., T. Ho, and M. W. Kirschner, "The Role of Microtubule Dynamics in Growth Cone Motility and Axonal Growth," *J. Cell Biol.*, **128**, 139 (1995).
Tanaka, E. M., and M. W. Kirschner, "Microtubule Behavior in the Growth Cones of Living Neurons During Axon Elongation," *J. Cell Biol.*, **115**, 345 (1991).
Toso, R. J., M. A. Jordan, K. W. Farrell, B. Matsumoto, and L. Wilson, "Kinetic Stabilization of Microtubule Dynamic Instability in Vitro by Vinblastine," *Biochemistry*, **32**, 1285 (1993).
Tran, P. T., and E. D. Salmon, "Microtubule Dynamic Instability is a Three-State Process," *Mol. Biol. Cell*, **4**, 165a (1993).
Vasquez, R. J., D. L. Gard, and L. Cassimeris, "XMAP from *Xenopus* Eggs Promotes Rapid Plus End Assembly of Microtubules and Rapid Microtubule Polymer Turnover," *J. Cell Biol.*, **127**, 985 (1994).
Verde, F., M. Dogterom, E. Stelzer, E. Karsenti, and S. Leibler, "Control of Microtubule Dynamics and Length by Cyclin A- and Cyclin B-Dependent Kinases in *Xenopus* Egg Extracts," *J. Cell Biol.*, **118**, 1097 (1992).
Walker, R. A., S. Inoue, and E. D. Salmon, "Asymmetric Behavior of Severed Microtubule Ends after Ultraviolet-Microbeam Irradiation of Individual Microtubules *in Vitro*," *J. Cell Biol.*, **108**, 931 (1989).
Walker, R. A., E. T. O'Brien, N. K. Pryer, M. F. Soboeiro, W. A. Voter, H. P. Erickson, and E. D. Salmon, "Dynamic Instability of Individual Microtubules Analyzed by Video Light Microscopy: Rate Constants and Transition Frequencies," *J. Cell Biol.*, **107**, 1437 (1988).
Yamada, K. M., B. S. Spooner, and N. K. Wessells, "Axon Growth: Roles of Microfilaments and Microtubules," *Proc. Nat. Acad. Sci. U.S.A.*, **66**, 1206 (1970).

Manuscript received Feb. 6, 1995, and revision received Aug. 10, 1995.